Green Synthesis and Antibacterial Effects of Silver Nanoparticles on Novel Activated Carbon

Ghadiri, Mohammad*+

Department of Chemistry, Faculty of Renewable Energies, Urmia University of Technology, Urmia, I.R. IRAN

Hallajzadeh, Jamal

Department of Biochemistry, Maragheh University of Medical Sciences, Maragheh, I.R. IRAN

Akhghari, Zahra

Department of Microbiology, Islamic Azad University –Qom Branch, Qom, I.R. IRAN

Nikkhah, Elhameh

[d]Medicinal Plants Research Center, Maragheh University of Medical Sciences, Maragheh, I.R. IRAN

Omar Othmn, Hazha •

Department of Chemistry, College of Science, Salahaddin University-Erbil, Erbil, Kurdistan region, IRAQ

ABSTRACT: *A green and simple method was proposed for the synthesis of silver nanoparticles (AgNPLs) on novel activated carbon (AC) using glucose and dextrin as reducer and stabilizer of silver ions. Semecarpus anacardium (SA) nutshells, an agricultural waste, were used as precursors to prepare low-cost activated carbon (AC) with a high surface area by chemical activation with KOH as an activator and different ratios of activating agent to precursor. Silver nanoparticles (AgNPLs) on AC samples were synthesized using chemical and green procedures. Silver nanoparticles (AgNPLs) on AC samples were synthesized using chemical and green procedures. Surface functional groups in Fourier transform infrared spectroscopy (FTIR) spectra and X-ray powder diffraction (XRD) diffractograms including a broad peak in the range of 2θ =15–28° and a weak and broad peak in the range of 2θ =40–48°, confirmed successful synthesis of AC. Also reduction of Ag^+ to Ag^0 and presence of Ag_2O was confirmed by XRD and SEM/EDX analysis. Scanning Electron Microscopes (SEM) reveals that the particles are spherical in shap and the Transmission Electron Microscopes (TEMs) images confirm the particle size distribution of the silver nanoparticles mainly in the range of 1–5 nm. EDX mapping used to observe the exact distribution of silver nanoparticles on the planar carbon surface. The BET results indicate that the AC synthesized with activating agent to precursor ratios of 1 has the highest surface area (717 $m^2 g^{-1}$) and the largest pore volume (0.286 $cm^3 g^{-1}$). Finally, the resulting Ag-AC was applied to study antimicrobial activity against gram-negative bacteria by Disk diffusion and the agar well method. Silver nanoparticles distributed on the activated carbon surface had significant antibacterial properties. The sample from green synthesis with an $AgNO_3$ solution concentration of 0.1 M showed the most antibacterial effect.*

KEYWORDS: *Activated Carbon; Green Synthesis; Semecarpus Anacardium; Ag Nano Particle; Antibacterial; Dextrin.*

**To whom correspondence should be addressed.*

+ E-mail: m.ghadiri@uut.ac.ir

• Other address: Pharmacy Department, Faculty of Pharmacy, Tishk International University, Erbil, Kursidtan region, IRAQ

1021-9986/2023/10/3198-3207 10/$/6.00

INTRODUCTION

Carbon materials have found versatile applications such as absorbents and molecular sieving, either as supports or as catalysts [1]. Activated carbon (AC) is the most efficient adsorbent used for pollutant removal due to its large surface area, well-developed pore structure, high-speed adsorption and thermal and chemical stability [2]. These useful and valuable adsorbents were produced from agricultural wastes such as fruit stones, peanuts, nutshells, bagasse, rice, oil palm waste, sawdust, and agricultural residues from sugarcane, of which millions of tonnes are produced annually [3]. Many important parameters, like the type and amount of activating agent, the production process, and the nature of the precursors, have a significant effect on the porosity and adsorption properties of the resultant AC. The production process includes chemical and physical steps. For the last method, a carbonaceous source is first carbonized under an inert atmosphere, and then the resulting char is activated at a high temperature by an oxidizing reagent such as steam. The chemical activation method commonly takes place at lower temperatures, and mesoporous ACs with a higher surface area are produced [2]. For this, carbonaceous precursors are merged at first with chemical reagents like some salts, alkali and acidic reagents and then the resulting slurry is heated at inert atmosphere.

Generally, chemical activation is more favored than the physical method because the chemical process has a lower carbonization temperature, shorter activation time and a simpler working process. During the last few years many researchers have reported chemical production of activated carbon from different agricultural wastes such as grape seeds by potassium carbonate (K_2CO_3) and potassium hydroxide (KOH) [4], peanut hull and olive stones by phosphoric acid [5, 6], date stones and wild chestnut shell by zinc chloride [7, 8]. These compounds can absorb pollutant molecules from both liquid and gas phases.

The prevalence of multidrug-resistant (MDR) among pathogens has become a global clinical problem for the eradication of bacterial infections and wants a new anti-infective. Silver nanoparticles are expected to play an increasingly important role in chemical, biochemical and biomedical researches and applications. They are important antibacterial materials as an effect of their larger surface areas in comparison to the bulk material. Researches have shown that silver nanoparticles, silver ions, and nano silver-containing complexes have antimicrobial behavior with a high ability to inactivate bacteria and viruses [9]. Silver nanoparticles were synthesized using chemical and green procedures. Reduction of silver ions using sodium borohydride ($NaBH_4$) is the most common method in chemical procedure. Studies showed that the morphology and size of synthesized silver nanoparticles can be controlled via the reducing agent [10]. In green procedures, natural compounds such as fruits extracts and glucose can be widely used due to their reducing properties, compatibility and eco-friendly [11].

Most recent studies shows that silver nanoparticles synthesized with Bougainvillea Glabra extract have significant antibacterial properties [10]. However ecofriendly Ag-NPs were recently synthesized by using piper cubeba seed extract and exhibited marked antimicrobial activity against various strains of gram negative and gram positive bacteria in addition to Candida albicans fungi [12].

This work investigates the preparation and characterization of activated carbon from *semecarpus anacardium* nutshell by KOH activation and novel green synthesis of Ag Nano particles on ACs using starch and glucose as stabilizing and reducing agents, respectively. The reason behind chosing semecarpus anacardium nutshell as an AC source is that scientific studies of the literature shown that activated carbon has not yet been produced from this source although it was produced from many agricultural wastes. After the synthesis of nanoparticles, we evaluated their antibacterial effects against E.coli. The results indicate that samples prepared by green method has the most antibacterial activity. To the best of our knowledge, no study was reported on antibacterial activity of Ag nanoparticles on activated carbon from semecarpus anacardium nutshell.

MATERIALS AND METHODS

Raw material and chemicals

Semecarpus anacardium (SA) used as raw materials for production of AC which collected from Kurdistan region in Iran. Potassium hydroxide (KOH, Merck) was applied as activating agent. Silver nitrate ($AgNO_3$, Merck, 99.8%), $NaBH_4$ (Merck), D (+)-Glucose monohydrate (Fulka) and Dextrin from corn (sigma-aldrich) were used for silver nanoparticle preparation. The *Escherichia coli* ATCC

25922 (Gram-negative) strain and Nutrient Broth (HIMEDIA) and Mueller-Hinton Agar (Biomaxima) culture mediums were used to Antibacterial test.

Synthesis of Activated Carbon

The chemical composition of the precursors influences the chemical properties of the activated carbons obtained at the same conditions [13,14]. Semecarpus Anacardium (SA) nutshells as a new precursor, were initially washed by hot water to remove water - soluble impurities, then placed in an oven to dry over night at 110°C. The dried precursor was sieved and sized to a particle size of 2mm. Postasium hydroxide was used as an activating agent for the merging step. The chemical ratio of activating agent/precursor was 1 to 3 in this study. The prepared samples were labeled C1, C2 and C3 for the ratios of 1, 2, and 3 respectively. In merging step the activating agent, nutshell precursor, and water were mixed via magnetic stirrer at 55°C for 24 hours. After mixing, the obtained slurry was dried in an oven at 110°C for 29 hours before becoming ready for the pyrolysis step.

The pyrolysis step was carried out in a N_2 atmosphere in a horizontal tube furnace 15 cm in height and 4 cm in diameter. The pyrolysis experiments were run by taking 10g of the merged sample under a N_2 flow rate of 200cm^3/min. The heating rate, final temperature, and maintenance time were 10°C/min, 600°C, and 60min respectively. After the carbonization, the sample was allowed to cool down to ambient temperature under N_2 gas. All AC samples were finely mixed in a 500 mL HCl solution (0.4N) and washed several times, first with hot and then with cold double distillated water, and finally oven dried at 110°C for 21 hours.

Preparation of AgNPs

Silver nanoparticles were synthesized via two procedures. For synthesis of AgC (chemical synthesize of silver nanoparticles via sodium borohydride and impregnation on AC), aqueous solutions (0.1M) of $AgNO_3$ were prepared in three erlenmeyers. Then 0.5 g of ACs were weighted and added in to each of the solutions. All samples were stirred for 70 hours in a dark place and then filtered and washed with double distilled water. Finally dried at 100 °C for 3 hours then the resulting products were dispersed in 20 mL of double distilled water followed by 8 mL sodium borohydride (0.2 M) as a reducing agent.

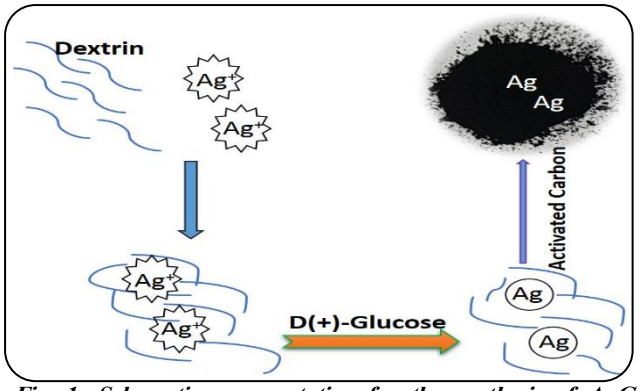

Fig. 1: Schematic representation for the synthesis of AgG nanoparticles

In order to prepare the AgG samples (Green synthesized via environmentally friendly material), firstly the dextrin solution (0.4 w/v) was prepared and mixed at constant temperature of 60 °C then 25 mL of $AgNO_3$ solution with different concentrations of 0.001M, 0.01M, 0.1M and 0.5M were added under continuous stirring for another 1h to obtain a homogenous solution. Subsequently, dextrin stabilized silver nanoparticles were synthesized by adding 1 mL D (+)-Glucose monohydrate solution. The mixture was stirred for 24 h to obtain a light brown color solution. Finally, 0.36 g of prepared AC samples were added into the solution and stirred for 24 h at 30 °C using a magnetic stirrer. The AgNPs were impregnated on ACs as green synthesis and named as Ag nanoparticle impregnated activated carbon (AgG). According to the literature, the optimum pH for green synthesis of nanoparticles is between 7 and 8.5. The pH value of double distilled water is in this range [10,12,15].

The samples are denoted as AgCx/y or AgGx/y where C and G stand for chemical and green synthesis, respectively, x represents the activating agent/precursor ratio and y represents the concentration of $AgNO_3$ solution. The prepared sample from green method with activating agent/precursor of 2 and $AgNO_3$ solution concentration of 0.1 M is labelled as AgG2/0.1. A schematic representation of the synthesis of silver nanoparticles loaded on the AC is shown in Fig. 1.

Characterization

The crystal structure of the samples was determined using X-ray power diffraction data obtained on a PHILIPS /PW1730, Netherlands diffractometer using CuKα radiation (λ= 1.5418 Å) as the X-ray source at 30 kV and

30 mA. The BET surface area and porosity of all AC samples were determined by N_2 adsorption/desorption measurements (BEL/ BELSORP MINI II, Japan) at 77 K. The surface functional groups of the samples were characterized using Fourier transform infrared spectrometer (FTIR, Thermo/AVATAR, USA) using KBr pellets containing 1 wt. % of the samples. The microscopic structure of the AgG2/0.1 sample was analyzed using a TEM CM120 (Netherlands) under an acceleration voltage of 100 kV. For morphology investigation, the scanning electron microscope (SEM) images are performed with TESCAN - MIRA III, Czechia equipped with energy-dispersive X-ray analysis (EDX) system and dot mapping on samples coated with gold to decrease charging.

Antimicrobial activity

The antibacterial effect of Ag nanoparticles was analyzed according to the recommendations of the National Committee for clinical laboratory standards (NCCLS) [16]. The *Escherichia coli* (E. coli) ATCC 25922 (Gram-negative) strain was used for the examing.

Disk diffusion and Agar Well Methods

Disk diffusion and agar well methods were used for the screening of antimicrobial activity in Ag nanoparticles. Bacterial suspensions were adjusted to match the turbidity of a 0.5 McFarland standard, yielding approximately 1.5×108 CFU/ mL. The bacteria spread with a sterile swab by moistening in bacterial suspension to prepare bacterial culture on Muller Hinton agar. In disk diffusion method some small and sterile filter paper disks of uniform size (6 mm) that were impregnated with 50 λ of each sample placed on the surface of an agar plate previously inoculated with a standard amount of E.coli separately. The disks were placed on the plate using a sterile forceps, at well-spaced intervals from each other. The plates were incubated at 37°C for 24 hours. After incubation time completed then the plates were tested for the presence of an inhibition zone around the antimicrobial disks. Subsequently, in agar well method, wells of 6 mm diameter were punched into the agar medium and filled with 100 µL of each sample. Then the plates were incubated in the upright position at 37℃ for 24 h. Wells containing the same volume of normal salin served as negative. The diameter of the inhibition zones around wells was measured based on millimeter after 24 hours [17].

MIC and MBC test

The MIC is the lowest concentration of an antimicrobial agent that inhibits the visible growth of a microorganism after overnight incubation [17]. The MICs of the samples were commonly determined for each strain by the macro dilution broth method as described by the NCCLS [18]. The serial dilutions of 1.25 mg/ mL concentration were prepared in microdilution tubes for each sample. Bacterial suspensions were adjusted to match the turbidity of a 0.5 McFarland standard, yielding approximately 1.5×10^8 CFU/mL. The same amount of bacteria was added to the test tubes. Then these tubes were incubated at 37 °C for 24 h. Each tube was examined for growth and compared to the control sample. The MBC is the lowest concentration of antibiotic required to kill a particular bacterium [19,20]. The 12 dilutions were run to perform the MBC test. The tubes were investigated to determining MIC values after 24 h of incubation. The MBC values were determined by sampling from all the macroscopically clear tubes after the first turbid tube in the series. Universally one dilution below the MIC was used for the levels to be assessed in the MBC assay [21].

RESULTS AND DISCUSSIOS

Morphology and Structures of ACS

The structures and morphologies of the prepared samples were analyzed by SEM. The resulting images for activated carbon (C2) and Ag nanoparticle containing AC (AgG2) are shown in Fig. 2. Its clear that the activated carbon surface was filled with pores and voids that may be formed by the release of gases produced by the decomposition of SA and salt chemical activation [22]. Previous studies have indicated that KOH interconnected in the internal structure of lignocellulosic materials, and it is used to prevent them from shrinking [23]. SEM images of AC-AgNPLs (Fig 2. b and c) confirm the sample heterogeneity and the irregular distribution of silver nanoparticles on the AC particle surfaces. This fact was also confirmed by EDX elemental analysis, as shown in Table 1.

EDX spectroscopy was also performed to investigate the elemental composition of Ag-NPs, which showed absorption peaks of silver at 3 Kv [12]. Other peaks also appeared for C, O, N, Cl, and Zn due to their presence in the AC and precursor materials. According to the SEM-EDX analysis, the composition of the elements in

Table 1: The surface area data, pore parameters and elemental analysis of samples

Sample	KOH/precursor (w/w)	S_{BET} ($m^2.g^{-1}$)	V_{tpore} (cm^3g^{-1})	V_m (cm^3g^{-1})	Mean pore diameter (nm)	Elemental analysis (wt%)					
						C	N	O	S	K	Ag
SA		-	-		-	44	11.3	44.1	0.08	0.52	0
C1	1	717.59	0.2863	164.87	1.5956	ND	ND	ND	ND	ND	ND
C2	2	647.25	0.3155	148.71	1.9495	72.2	14.5	12.5	0.17	0.62	0
C3	3	557.11	0.3112	128	2.2344	ND	ND	ND	ND	ND	ND
AgG2/0.1 (ı)		ND	ND	ND	ND	74.74	4.02	15.24	ND	ND	4.48
AgG2/0.1 (ıı)		ND	ND	ND	ND	71.66	4.25	20.12	ND	ND	3.02

S_{BET}: BET Surface Area, V_{tpore}: total pore volume, V_m: monolayer volume, ND: no detected
AgG2/0.1 (ı) and AgG2/0.1 (ıı): Elemental analysis according to the Fig.2 (b).

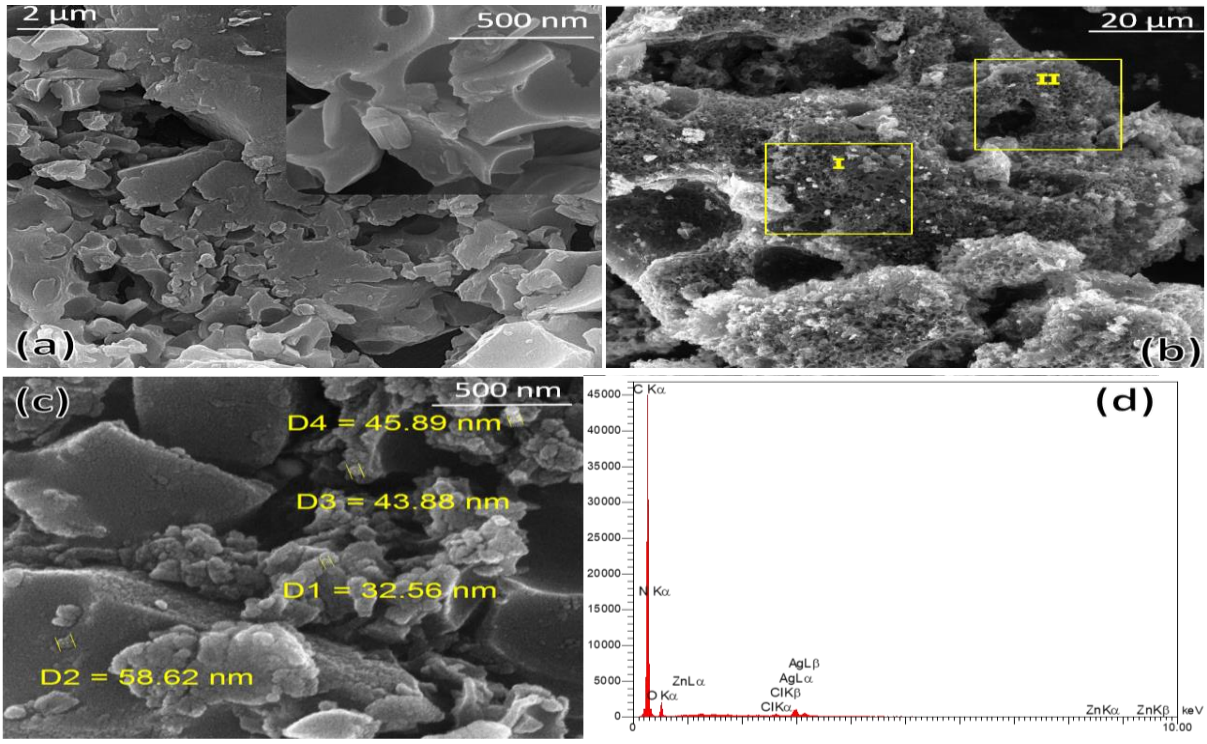

Fig. 2: SEM images of C2 (a), and AgG2/0.1 samples (b and c) and EDX spectrum of AgG2/0.1 sample

AgG2/0.1 at the point ı was as follows: 74.74% for carbon, 15.24% for oxygen, 4.02% for nitrogen, 1.5% for chlorine and zinc, and 4.48% for silver. Depending on the results, it emphasized that silver nanoparticles were successfully reduced and dispersed on AC. The specific BET surface areas, total and monolayer pore volumes and pore diameters of the prepared ACs in this study are summarized in Table 1. As shown all the samples have relatively high surface areas, indicating well-developed pore structures. In addition, the surface area and monolayer volume pore volumes of the samples were decreased by increasing the activating agent/precursor ratio. The total pore volume did not change significantly when the KOH/wood ratio was changed in the C2 and C3 samples.

As a representative example, TEM micrographs of AgG2/0.1 sample is shown in Fig. 3(a–b). The characterized silver nanoparticles are nearly spherical with uniform particle morphology. A higher magnification result demonstrates that the particle size distribution of sample is mainly in the range of 1–5 nm. Recent studies have found that the produced silver nanoparticles were predominantly spherical in morphology, and ranged from

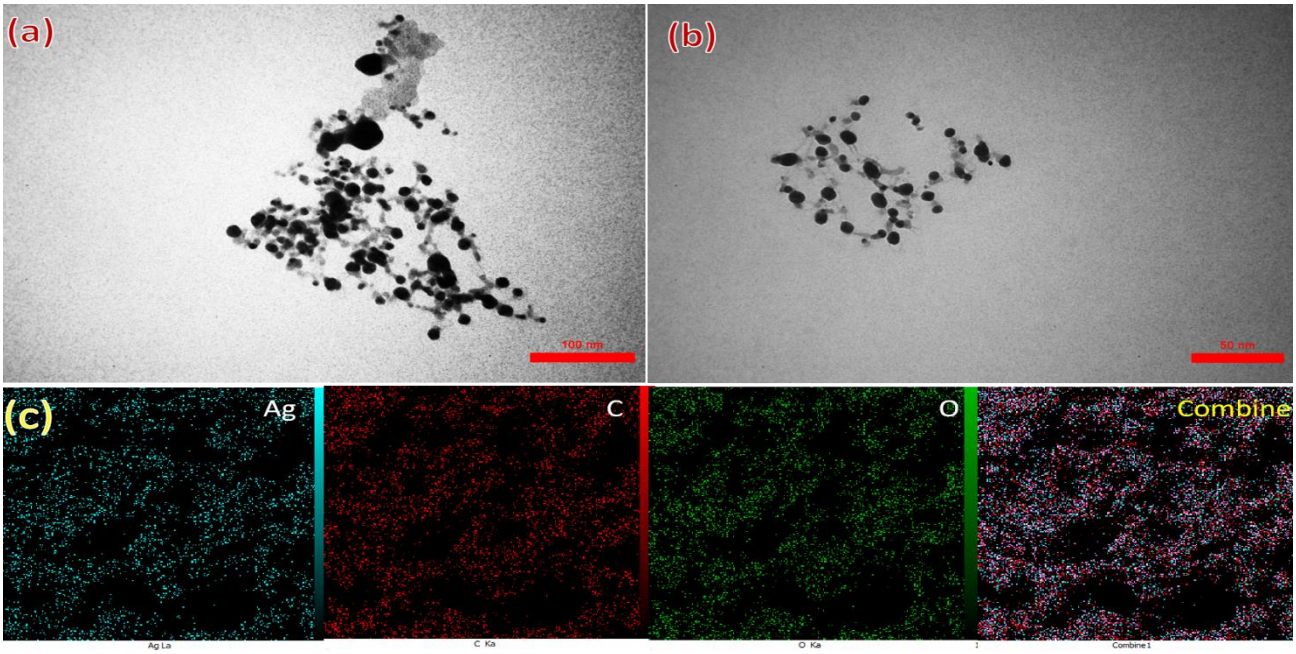

Fig. 3: TEM images of: (a-b) AgNPLs in AgG2/0.1 sample , (c) EDS elemental mapping images of AgG2/0.1 sample

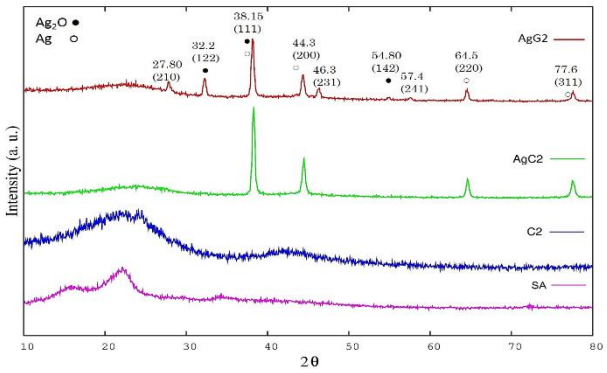

Fig. 4: XRD spectrum of semecarpus anacardium (SA) nutshells, activated carbon (C2) and AC loaded silver nanoparticles

1 to 40 nm and 1–25 nm in diameter [15]. TEM images show that the AgG2/0.1 sample has well-dispersed particles of nano-sized silver particles as dark areas homogeneously dispersed with particle size distribution mainly in the range of 1–5 nm. The EDS elemental mapping images of AgG2/0.1 sample were shown in Fig. 3(c) and indicated that the sample consisted of three main elements: carbon, oxygen and silver which were homogenous distributed throughout the sample, confirming that the blue dots were composed of AgNPs, red dots were activated carbon (AC) and green dots were oxygen (O).

Fig. 4 shows the XRD patterns of SA, C2, AgC2, and AgG2 samples. The relatively distinct diffraction peak of SA shell sample at about 2θ =16◦ and 34◦ compared to that of obtained C2 activated carbon indicates complete carbonization and AC production with highly amorphous nature. The XRD patterns of prepared AC sample (C2) exhibited a broad peak in the range of 2θ =15–28° and a weak and broad peak in the range of 2θ =40–48° diffraction related to (002) and (100) planes, and these diffractions can be attributed to the randomly arranged amorphous carbon structures with carbon rings that disorderly stack up due to the low content of crystalline graphite, respectively [24,25].

The XRD pattern indicates the four main diffraction peaks at 2θ values of 38.15°, 44.3°, 64.5° and 77.6° attributed to the (111), (200), (220) and (311) crystallographic planes of the face centered cubic (FCC) Ag (JCPDS card no. 65-2871) [21]. X-ray diffraction results of AgC2 sample clearly show that Ag^+ ions have been successfully reduced by the Sodium borohydride and it is crystalline in nature [26]. AgG2 sample shows other characteristic diffraction peaks at 32.2°, 38.15° and 54.8° at 2θ scale which could be indexed to (122), (200) and (220) peaks, respectively, that are assigned to cubic Ag_2O (JCPDS 41-1104). The (122) peak of Ag_2O which is the first most intense peak at 32.2° indicates that the content of Ag_2O nanoparticles and nano sheets is much less than that of Ag. The graph also includes the location of Ag

Table 2: Antibacterial effect of the Ag-nanoparticles by disk diffusion and agar well methods

Test samples		AgC1/0.1	AgC2/0.1	AgC3/0.1	AgG2/0.1	C2	AgG2/0.5	AgG2/0.01	AgG2/0.001	Blank
E.coli	Disk diffusion	8	13	12	15	9	15	14	13	-
	Agar well	7	12	12	14	9	14	13	13	-

Results are expressed in mm. Blank (normal saline as solvent of nanoparticles)

Table 3: The Minimum Inhibition Concentration (MIC) and Minimum Bactericidal Concentration (MBC) of Ag-nanoparticles

Test samples		AgC2/0.1	AgC3/0.1	AgG2/0.1
E.coli	MIC	0.0195	0.078	0.078
	MBC	0.039	0.156	0.156

MIC and MBC values are expressed in mg/ mL.

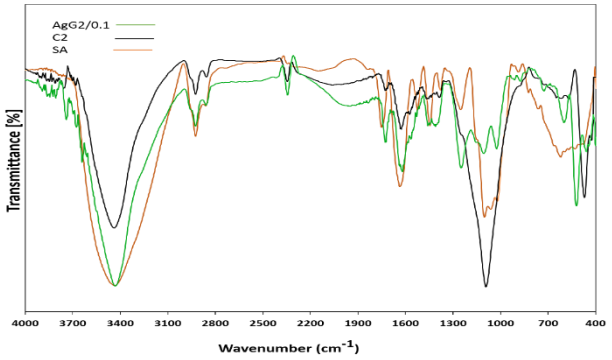

Fig. 5: FT-IR spectra of semecarpus anacardium (SA) nutshells, activated carbon (C2) and AgG2/0.1 nanoparticles

crystal peaks, it suggests that the prepared samples were the mixtures of Ag/Ag_2O nanocomposites. On the other hand, different crystallinity and phases of Ag nanoparticles, were identified as evidenced by the unassigned peaks at 2θ values of 27.8°, 46.3° and 57.4° corresponding to (210), (231) and (241) planes, respectively (as correlated to JCPDS: File No.4-783), is thought to be related to other Ag nano crystalline phases and suggests that the prepared silver nanoparticles were biphasic in this sample [27-29]. The presence of a strain in the crystal structure causes a slight shift in the peak positions.

FTIR spectroscopy was applied for the study of the functional groups and chemical composition of the samples. Fig. 5 explains the FTIR spectra of SA, C2, and AgG2/0.1 samples in the range of 450-4000 cm^{-1}. The SA nutshell and prepared AC (C2) samples showed four major absorption bands at 2900-3500 cm^{-1}, 1300-1730 cm^{-1}, 1000-1250 cm^{-1} and 450-700 cm^{-1}. A broad stretching band at around 3420 cm^{-1} is mainly caused by the hydroxyl groups vibration of the adsorbed water molecules on the surface of nutshells and AC after carbonization. Absorption peaks appearing at 2850 to 2925 cm^{-1} for these samples suggests the presence of CH stretching vibration and CH_2 asymmetrical vibrations.

The band at around 1626 cm^{-1} in C2 activated carbon is ascribed to the C=O stretching vibration, which decreased in comparison to the raw material due to the dehydrating impact of KOH [30]. Weak band at 1524 cm^{-1} for SA nutshell samples indicate the presence of C=C bonds of aromatic compounds and after carbonization cannot be seen for C2 activated sample [31].

The FTIR spectrum of synthetic carbon C2 at around 1454 cm^{-1} shows absorption bands due to –CH– deformation. The broad band observed in the region of 1000 to 1250 cm^{-1} was assigned due to a characteristic absorption of hydroxyl (–OH) group. These results are in good agreement with that in other investigators. Peaks around the 480-485 cm^{-1} are associated with the in plane and out-of-plane aromatic ring deformation vibrations [32].

In both C2 and AgG2/0.1 samples, peaks marked with chemical bonds appear at the same frequencies. This indicates that the incorporation of AgNPs does not lead to changes in the chemical bonds and composition.

Antibacterial efficacy results

The results from antibacterial tests showed that Ag-nanoparticles synthesis by various methods has antibacterial activity (Fig. 6). The results of the disk diffusion and agar well methods are shown in Table 2. Among all samples, the AgC1/0.1 had poor activity, unlike AgG2/0.1 that showed the most antibacterial activity. The Minimum Inhibition Concentration (MIC) and Minimum Bactericidal Concentration (MBC) of Ag-nanoparticles are listed in Table 3.

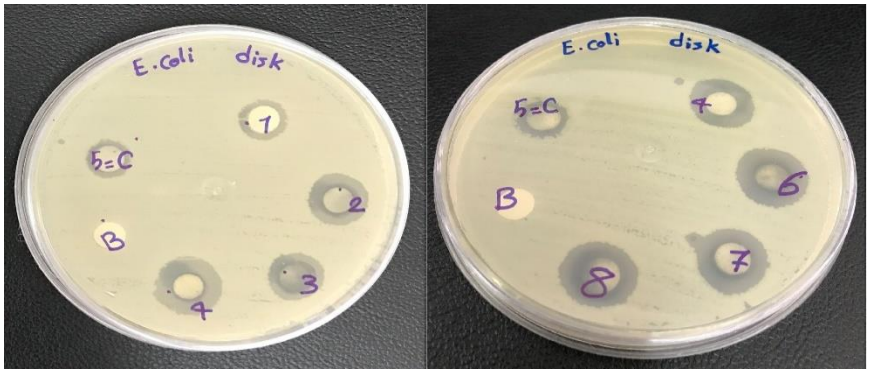

Fig.6: Inhibition Zone of samples against E.coli (mm) in disk diffusion method. AgC1/0.1 (1), AgC2/0.1 (2), AgC3/0.1 (3), AgG2/0.1 (4), C2 (5), AgG2/0.5 (6), AgG2/0.01 (7), AgG2/0.001 (8), and B (Blank)

CONCLUSION

Brifly a series of activated carbon materials with high specific surface area were synthesized by KOH chemical activation from *semecarpus anacardium* nutshell as agricultural wastes. Then, silver nanostructures were effectively imbued onto ACs via chemical and green synthesis, utilizing glucose as a reducing agent for the starch-stabilized approach. Samples characterized by XRD, SEM/EDX, FTIR, and Brunauer, Emmett and Teller (BET) surface area and TEM techniques shows formation of activated carbon and silver nanoparticles over planner AC sheets. The average diameter of the silver nanoparticles was mainly in the range of 1 to 5 nm. Studies shown that the samples prepared by green method has more antibacterial effects than that one prepared by the chemical method. Furthermore, samples based on activated carbons with high specific surface area and large pore volume and containing silver nanoparticles and mixtures of Ag/Ag_2O nanocomposites revealed growth inhibition zones against *Escherichia coli* and exhibited good antimicrobial activity, which is probably due to its large surface area and small size and spherical shape of silver nanoparticles. The material obtained through this novel approach may be a promising agent for application for environmental and biomedical applications, which will be explored in the near future.

Acknowledgements

The authors gratefully acknowledge Urmia University of Technology and Maragheh University of Medical Sciences for financial support.

Received : Dec. 22, 2022 ; Accepted : Apr. 17, 2023

REFERENCES

[1] Chen Y., Zhu Y., Wang Z., Li Y., Wang L., Ding L., et al. Application Studies of Activated Carbon Derived from Rice Husks Produced by Chemical-Thermal Process—A Review, *Advances in colloid and interface science*, **163(1)**: 39-52 (2011).

[2] Aljeboree AM., Alshirifi AN., Alkaim AF., Kinetics and Equilibrium Study for the Adsorption of Textile Dyes on Coconut Shell Activated Carbon, *Arabian journal of chemistry*, **10:** S3381-S3393 (2017).

[3] Mohanty K., Jha M., Meikap B., Biswas M., Preparation and Characterization of Activated Carbons from Terminalia Arjuna Nut with Zinc Chloride Activation for the Removal of Phenol from Wastewater, *Industrial & engineering chemistry research*, **44(11)**: 4128-4138 (2005).

[4] Krishnamoorthy R., Govindan B., Banat F., Sagadevan V., Purushothaman M., Show PL., Date Pits Activated Carbon for Divalent Lead Ions Removal, *Journal of bioscience and bioengineering*, **128(1)**: 88-97 (2019).

[5] Zafar, M., Ghafoor, S., Tabassum, M., Zubair, M., Nazar, M., Ashfaq, M., Utilization of Peanut (Arachis hypogaea) Hull Based Activated Carbon for the Removal of Amaranth Dye from Aqueous Solutions, *Iranian Journal of Chemistry and Chemical Engineering*, **39(4)**: 183-191 (2020).

[6] Elazzouzi M., Haboubi K., Elyoubi M., Electrocoagulation Flocculation as a Low-Cost Process for Pollutants Removal from Urban Wastewater, *Chemical Engineering Research and Design*, **117**: 614-626 (2017).

[7] Ahmed M.J., Theydan S.K., Physical and Chemical Characteristics of Activated Carbon Prepared by Pyrolysis of Chemically Treated Date Stones and its Ability to Adsorb Organics, *Powder technology*, **229**: 237-245 (2012).

[8] Altintig E., Kirkil S., Preparation and Properties of Ag-Coated Activated Carbon Nanocomposites Produced from Wild Chestnut Shell by $ZnCl_2$ Activation, *Journal of the Taiwan institute of chemical engineers*, **63**: 180-188 (2016).

[9] Catalano P.N., Pezzoni M., Costa C., Soler GJdAA., Bellino M.G., Desimone M.F., Optically Transparent Silver-Loaded Mesoporous thin Film Coating with Long-Lasting Antibacterial Activity, *Microporous and Mesoporous Materials*, **236**: 158-166 (2016).

[10] Momeni M., Asadi S., Shanbedi M., Antimicrobial Effect of Silver Nanoparticles Synthesized with Bougainvillea Glabra Extract on Staphylococcus Aureus and Escherichia Coli, *Iranian Journal of Chemistry and Chemical Engineering*, **40**(2): 395-405 (2021).

[11] Archana C., Iftkhar A., Preeti S., Mehraj Ud Din S., Gulshitab A., Suresh S., et al., Green Synthesis of Silver Nanoparticles Using Fruits Extracts of Syzygium Cumini and their Bioactivity, *Chemical Physics Letters*, **759**: 139493-139498 (2022).

[12] Magdy G., Aboelkassim E., El-Domany R.A. et al., Green Synthesis, Characterization, and Antimicrobial Applications of Silver Nanoparticles as Fluorescent Nanoprobes for the Spectrofluorimetric Determination of Ornidazole and Miconazole, *Scientific Reports*, **12**: 21395 (2022).

[13] Hassan M.F., Sabri M.A., Fazal H., Hafeez A., Shezad N., Hussain M., Recent Trends in Activated Carbon Fibers Production from Various Precursors and Applications—A Comparative Review, *Journal of Analytical and Applied Pyrolysis*, **145**: 1118–1125 (2020).

[14] Yunus Z. M., Al-Gheethi A., Othman N., Hamdan R., Ruslan N. N., Advanced Methods for Activated Carbon from Agriculture Wastes; A Comprehensive Review, *International Journal of Environmental Analytical Chemistry*, **102(1)**: 134-158 (2022).

[15] Alharbi N.S., Alsubhi N.S., Felimban, A.I., Green Synthesis of Silver Nanoparticles Using Medicinal Plants: Characterization and Application, *Journal of Radiation Research and Applied Sciences*, **15(3)**: 109-124 (2022).

[16] Humphries R.M., Ambler J., Mitchell SL., Castanheira M., Dingle T., Hindler J.A., et al., CLSI Methods Development and Standardization Working Group Best Practices for Evaluation of Antimicrobial Susceptibility Tests, *Journal of clinical microbiology*, **56(4)**:01934-17 (2018).

[17] Dahiya P., Purkayastha S., Phytochemical Screening and Antimicrobial Activity of Some Medicinal Plants Against Multi-Drug Resistant Bacteria from Clinical Isolates, Indian Journal of Pharmaceutical Sciences, **74(5)**: 443-450 (2012).

[18] CLSI. Performance Standards for Antimicrobial Disk Susceptibility Tests; Approved Standard. Edition E, editor. Wayne, PA: Clinical and Laboratory Standards Institute; (2012).

[19] Limoncu M.H., Ermertcan Ş., Erac B., Taşli H., An Investigation of the Antimicrobial Impact of Drug Combinations Against Mycobacterium Tuberculosis Strains, *Turkish Journal of Medical Sciences*, **41(4)**: 719-724 (2011).

[20] Fekri M. H., Tousi F., Heydari R., Razavi Mehr M., Rashidipour M., Synthesis of Magnetic Novel Hybrid Nanocomposite (Fe_3O_4@SiO_2/Activated Carbon) by a Green Method and Evaluation of Its Antibacterial Potential, *Iranian Journal of Chemistry and Chemical Engineering*, **41(3)**: 767-776 (2022).

[21] Yilmaz M.T., Minimum Inhibitory and Minimum Bactericidal Concentrations of Boron Compounds Against Several Bacterial Strains, *Turkish Journal of Medical Sciences*, **42(Sup. 2)**: 1423-1429 (2012).

[22] Gong Y., Wang H., Wei Z., Xie L., Wang Y., An Efficient Way to Introduce Hierarchical Structure into Biomass-Based Hydrothermal Carbonaceous Materials., *ACS Sustainable Chemistry & Engineering*, **2(10)**: 2435-2441 (2014).

[23] Danish M., Ahmad T., A Review on Utilization of Wood Biomass as a Sustainable Precursor for Activated Carbon Production and Application, *Renewable and Sustainable Energy Reviews*, **87**: 1-21 (2018).

[24] Tang Y-B., Liu Q., Chen F-Y., Preparation and Characterization of Activated Carbon from Waste Ramulus Mori, *Chemical Engineering Journal*, **203**: 19-24 (2012).

[25] Zhao J., Yang L., Li F., Yu R., Jin C., Structural Evolution in the Graphitization Process of Activated Carbon by High-Pressure Sintering, *Carbon*, **47(3)**: 744-751 (2009).

[26] Khan M., Khan M., Adil SF., Tahir MN., Tremel W., Alkhathlan HZ., et al., Green Synthesis of Silver Nanoparticles Mediated by Pulicaria Glutinosa Extract, *International journal of nanomedicine*, **8**: 1507-1516 (2013).

[27] Jayaseelan C., Rahuman A.A., Acaricidal Efficacy of Synthesized Silver Nanoparticles Using Aqueous Leaf Extract of Ocimum Canum Against Hyalomma Anatolicum Anatolicum and Hyalomma Marginatum Isaaci (Acari: Ixodidae), *Parasitology research*, **111**(3): 1369-1378 (2012).

[28] Awwad A.M., Salem N.M., Abdeen A.O., Green Synthesis of Silver Nanoparticles Using Carob Leaf Extract and its Antibacterial Activity, *International journal of Industrial chemistry*, **4(1)**: 29 (2013).

[29] Yan Z., Bao R., Chrisey D.B., Generation of Ag–Ag_2O Complex Nanostructures by Excimer Laser Ablation of Ag in Water, *Physical Chemistry Chemical Physics*, **15(9)**: 3052-3056 (2013)

[30] Zhong Z-Y., Yang Q., Li X-M., Luo K., Liu Y., Zeng G-M., Preparation of Peanut Hull-Based Activated Carbon by Microwave-Induced Phosphoric Acid Activation and its Application in Remazol Brilliant Blue R Adsorption, *Industrial Crops and Products*, **37(1)**: 178-185 (2012).

[31] Hsu C.F., Zhang L., Peng H., Travas-Sejdic J., Kilmartin P.A., Free Radical Scavenging Properties of Polypyrrole and Poly (3, 4-Ethylenedioxythiophene), *Current Applied Physics*, **8(3-4)**: 316-319 (2008).

[32] Attia A.A., Rashwan W.E., Khedr S.A., Capacity of Activated Carbon in the Removal of Acid Dyes Subsequent to its Thermal Treatment., *Dyes and Pigments*, **69(3)**: 128-136 (2006).